Neurochemistry International 129 (2019) 104498

Contents lists available at ScienceDirect

Neurochemistry International

journal homepage: www.elsevier.com/locate/neuint

Different responses of PC12 cells to different pro-nerve growth factor protein variants

Marzia Soligo[a], Martina Albini[a], Federico Lorenzo Bertoli[a], Valeria Marzano[b], Virginia Protto[a], Luisa Bracci-Laudiero[a,c], Gaetana Minnone[c], Fabrizio De Benedetti[c], Antonio Chiaretti[d], Elide Mantuano[a], Luigi Manni[a,*]

[a] Institute of Translational Pharmacology, Consiglio Nazionale Delle Ricerche (CNR), Rome, Italy
[b] Human Microbiome Unit, Genetic and Rare Diseases Area, Bambino Gesù Children's Hospital IRCCS, Rome, Italy
[c] Division of Rheumatology and Immuno-Rheumatology Research Laboratories, Bambino Gesù Children's Hospital, Rome, Italy
[d] Institute of Pediatrics, Università Cattolica del Sacro Cuore, Rome, Italy

ARTICLE INFO

Keywords:
Pro-nerve growth factors
PC12 cells
Ngf gene expression
Tropomyosine receptor kinase A
p75 neurotrophin receptor

ABSTRACT

The present work aimed to explore the innovative hypothesis that different transcript/protein variants of a pro-neurotrophin may generate different biological outcomes in a cellular system. Nerve growth factor (NGF) is important in the development and progression of neurodegenerative and cancer conditions. Mature NGF (mNGF) originates from a precursor, proNGF, produced in mouse in two major variants, proNGF-A and proNGF-B. Different receptors bind mNGF and proNGF, generating neurotrophic or neurotoxic outcomes. It is known that dysregulation in the proNGF/mNGF ratio and in NGF-receptors expression affects brain homeostasis. To date, however, the specific roles of the two major proNGF variants remain unexplored. Here we attempted a first characterization of the possible differential effects of proNGF-A and proNGF-B on viability, differentiation and endogenous *ngf* gene expression in the PC12 cell line. We also investigated the differential involvement of NGF receptors in the actions of proNGF. We found that native mouse mNGF, proNGF-A and proNGF-B elicited different effects on PC12 cell survival and differentiation. Only mNGF and proNGF-A promoted neurotrophic responses when all NGF receptors are exposed at the cell surface. Tropomyosine receptor kinase A (TrkA) blockade inhibited cell differentiation, regardless of which NGF was added to culture media. Only proNGF-A exerted a pro-survival effect when TrkA was inhibited. Conversely, proNGF-B exerted differentiative effects when the p75 neurotrophin receptor ($p75^{NTR}$) was antagonized. Stimulation with NGF variants differentially regulated the autocrine production of distinct proNgf mRNA. Overall, our findings suggest that mNGF and proNGF-A may elicit similar neurotrophic effects, not necessarily linked to activation of the same NGF-receptor, while the action of proNGF-B may be determined by the NGF-receptors balance. Thus, the proposed involvement of proNGF/NGF on the development and progression of neurodegenerative and tumor conditions may depend on the NGF-receptors balance, on specific NGF trancript expression and on the proNGF protein variant ratio.

1. Introduction

Nerve growth factor (NGF) is translated from two major alternatively spliced transcripts to produce 34 and 27 kDa pre-proNGFs. In the endoplasmic reticulum the removal of the pre-pro signal sequences results in two proNGF species, proNGF-A and proNGF-B, with molecular masses of 32 and 25 kDa respectively (Edwards et al., 1986). In 2001, Lee et al. shattered the traditional view that the precursor-NGF is functionally inactive, showing that secreted proNGF promotes cell death (Lee et al., 2001). Subsequent studies demonstrated that in brain tissues proNGF is the predominant form of NGF. Indeed, whereas mNGF is undetectable, proNGF synthesis is increased in the brain of Alzheimer's disease patients (Fahnestock et al., 2001) and its secretion is enhanced following brain injury (Beattie et al., 2002; Harrington et al., 2004). Moreover, increased proNGF levels and activity have been reported in neoplastic diseases such as breast and prostate cancer,

Abbreviations: CNS, central nervous system; NGF, nerve growth factor; mNGF, mature NGF; proNGF, NGF precursor; $p75^{NTR}$, p75 neurotrophin receptor; SMG, submaxillary glands; TrkA, Tropomyosine receptor kinase A

* Corresponding author. Institute of Translational Pharmacology, National Research Council of Italy (CNR), via del Fosso del Cavaliere 100, 00133, Rome, Italy.
E-mail address: luigi.manni@ift.cnt.it (L. Manni).

https://doi.org/10.1016/j.neuint.2019.104498
Received 13 March 2019; Received in revised form 24 May 2019; Accepted 1 July 2019
Available online 03 July 2019
0197-0186/

positively correlated with high levels of tumorigenesis and tumor cell invasion (Bradshaw et al., 2015; Demont et al., 2012).

When the p75 neurotrophin receptor ($p75^{NTR}$)/sortilin complex is activated, proNGF acts as pro-apoptotic factor (Nykjaer et al., 2004). Activation of $p75^{NTR}$ alone or of the $p75^{NTR}$/tropomyosin receptor tyrosine kinase A (TrkA) complex leads to proNGF-induced pro-survival and/or differentiative effects, similar to those induced by mNGF (Hempstead, 2014). Thus, the relative levels of proNGF and mNGF receptors could determine the pro-apoptotic or neurotrophic activity of proNGF (Masoudi et al., 2009). Moreover, the study of the ratio between proNGF and mNGF and the dynamics of proNGF-to-mNGF conversion is gaining increasing importance (Bruno and Cuello, 2006). Alterations in mNGF/proNGF physiological dynamics could affect the progression of neurodegeneration in diseases such as diabetic encephalopathy (DE) (Soligo et al., 2015) or Alzheimer's disease (AD) (Bruno and Cuello, 2006; Capsoni and Cattaneo, 2006; Chao et al., 2006; Cuello and Bruno, 2007; Cuello et al., 2010; Fahnestock et al., 2001; Iulita and Cuello, 2014).

There are already clues that proNGF-A and proNGF-B may have different biological functions (Protto et al., 2019; Soligo et al., 2015). It is therefore reasonable to suggest that the ratio between proNGF-A and proNGF-B should be investigated when studying the involvement of the proNGF/mNGF system in the development and progression of diseases. The aim of the present study was to provide a first characterization of the specific biological actions of the different proNGF protein variants using the well-characterized PC12 cells *in vitro* model (Greene, 1978; Masoudi et al., 2009; Rudkin et al., 1989). The different proNGF protein variants were purified from mice SMG and verified by mass spectrometry analysis. We then investigated their selective effects on cell viability and differentiation and analyzed the roles of the different NGF receptors in mediating their functions. We also studied endogenous Ngf mRNA expression in response to stimulation with proNGF and we isolated and sequenced rat proNgf-A mRNA, the presence of which had previously only been predicted by bioinformatics and genome analysis.

2. Methods

2.1. Purification of native mouse proNGF isoforms

Fifty grams of submaxillary glands (SMG) from adult male CD-1 mice were homogenized in 20 mM sodium phosphate buffer, pH 7.0 (homogenization buffer) in a pre-chilled glass blender, at a 1:5 ratio (weight/volume). After centrifugation for 30 min at 10000 × *g*, the supernatant was added to a diethylaminoethanol (DEAE) Sepharose FF medium (250 ml; GE Healthcare) packed in a XK 26/70 column (GE Healthcare) equilibrated with the homogenization buffer. After washing the DEAE medium in 10 vol of buffer, a linear gradient from 0 to 1M NaCl in 20 column volumes was applied and DEAE fractions I-IV (Fig. 1A) collected and analyzed by SDS-PAGE followed by Western blot (Fig. 1B). Fraction DEAE-II was then dialyzed O.N. against sodium phosphate buffer pH 7.0 + 1 mM EDTA (phenyl sepharose, PS buffer). At the end of the dialysis, $(NH_4)_2SO_4$ at a final 1M concentration was added to the DEAE-II fraction, which was then loaded on a 16/10 prepacked phenyl sepharose (PS) column (GE Healthcare) equilibrated with PS buffer + 1M $(NH_4)_2SO_4$. After washing, a $(NH_4)_2SO_4$ linear gradient from 1M to 0M was applied to the column (Fig. 1C). PS fractions I-IV were collected and analyzed as described above. Semi-purified proNGFs with molecular weight around 27 and 32–34 kDa were detected in PS-III and PS-IV fractions respectively (Fig. 1C and D). PS-III and PS-IV fractions were dialyzed O.N. against ultrapure water and then lyophilized in 0.15 mg aliquots and stored at −80 °C. The final purification step was size-exclusion chromatography performed by a Superdex 75 pg medium prepacked into a XK 10/70 column (GE Healthcare, total volume: V_t = 120 ml). The column was calibrated by Blue Dextran (0.1 mg/ml), RNAseA (MW: 13 kDa), carbonic anidrase (MW: 29 kDa) and ovalbumin (MW: 43 kDa) (chromatogram not shown). According to the obtained retention volumes, a void volume (V_0) of 42 ml was calculated, together with the partition coefficient (Kav) for the calibration proteins and the equation relative to the selectivity curve (Kav = 0.215*ln(MW) + 2.56, R^2 = 0.9993) that allows the prediction of Kav and elution volumes [V_e = Kav*(V_t-V_0)-V_0] for the proNGFs to be purified. The lyophilized proNGFs were then suspended in 25 mM sodium phosphate (PB) pH 5.6, 0.1 M NaCl, 4 M urea and injected into the column (Fahnestock et al., 2004b). The column was eluted with the same buffer, peaks were collected and assayed by Coomassie staining and Western blot (proNGF-A: Fig. 1E and F, proNGF-B: Fig. 1G and H). Fractions containing proNGF were dialyzed against ultrapure water to remove urea, lyophilized and stored at −80 °C.

2.2. Proteomic analysis of purified proNGFs

Lyophilized samples were resuspended in 50 mM ammonium bicarbonate and trypsin digestion was performed after reduction with 10 mM DTT and alkylation with 20 mM iodoacetamide (IAA). Protein samples were digested 50:1 (w/w) with sequence grade trypsin (Promega, Madison, WI, USA) at 37 °C overnight. The reaction was stopped by adding a final concentration of 0.1% formic acid (FA). The peptides, desalted by reverse phase extraction using StageTip C18 (Sigma-Aldrich, Milan, Italy) (Rappsilber et al., 2007) were resuspended with 2% acetonitrile (ACN), 0.1% FA and analyzed by nano liquid chromatography-electrospray-tandem mass spectrometry (nLC-ESI-MS/MS) on a hybrid quadrupole-Orbitrap Q Exactive HF mass spectrometer (Thermo Fisher Scientific, Waltham, MA, USA) (Soffientini and Bachi, 2016). Protein identifications were obtained by processing MS data with MaxQuant software (v. 1.5.8.3, Max-Planck-Institut für Biochemie - Max-Planck-Gesellschaft, Munich) and searching with the embedded Andromeda search engine against UniProtKB Protein Knowledgebase (release 2018_05, taxonomical restriction Mus musculus) with the following parameters: enzyme trypsin; maximum missed cleavage 2; fixed modification: carbamidomethylation of cysteine; variable modifications: oxidation of methionine and protein N-terminal acetylation; fragment ion mass tolerance 40 ppm and parent ion tolerance 0.006 Da, minimum 2 peptides matched per protein, and false discovery rate under 0.01 (i.e.: the expected fraction of incorrect peptide spectrum match in the entire data set is less than 1%, calculated on a decoy database).

2.3. Cell culture

PC12 cells were grown in RPMI 1640 supplemented with 10% horse serum and 5% calf serum (complete-medium; Invitrogen Life Technologies) in a humidified atmosphere of 5% CO_2 at 37 °C. In these culture conditions, PC12 cells display the characteristics of exponentially-growing cells (Greene and Tischler, 1976). PC12 cells were also primed in complete-medium supplemented with 50 ng/ml of murine mNGF, produced in our laboratory as previously described (Chiaretti et al., 2017) (supplemented-medium) for 10–14 days before harvesting (Greene and Tischler, 1976; Seeley et al., 1983). PC12 cells, for use in bioassays, were washed three times in serum-free medium and incubated with equimolar (8 nM) amounts of mNGF (100 ng/ml), proNGF-A (250 ng/ml) or proNGF-B (200 ng/ml), for the indicated times in serum-free medium. The different protein variants were added to cell culture every day to limit the effects of degradation of the stimuli. For the indicated experiments, primed PC12 cells were pre-treated for 30-min with 2 μg/ml of rhTrkA/Fc Chimera (cat. 175-TK, R&D systems, Minneapolis, MN, USA), able to block NGF-dependent neuritogenesis in PC12 cells (Marsh et al., 2002) or 10 mM $p75^{NTR}$ inhibitor (LM11A-31, cat. SML0664, Sigma Aldrich) (Massa et al., 2006) before incubation with mNGF/proNGFs.

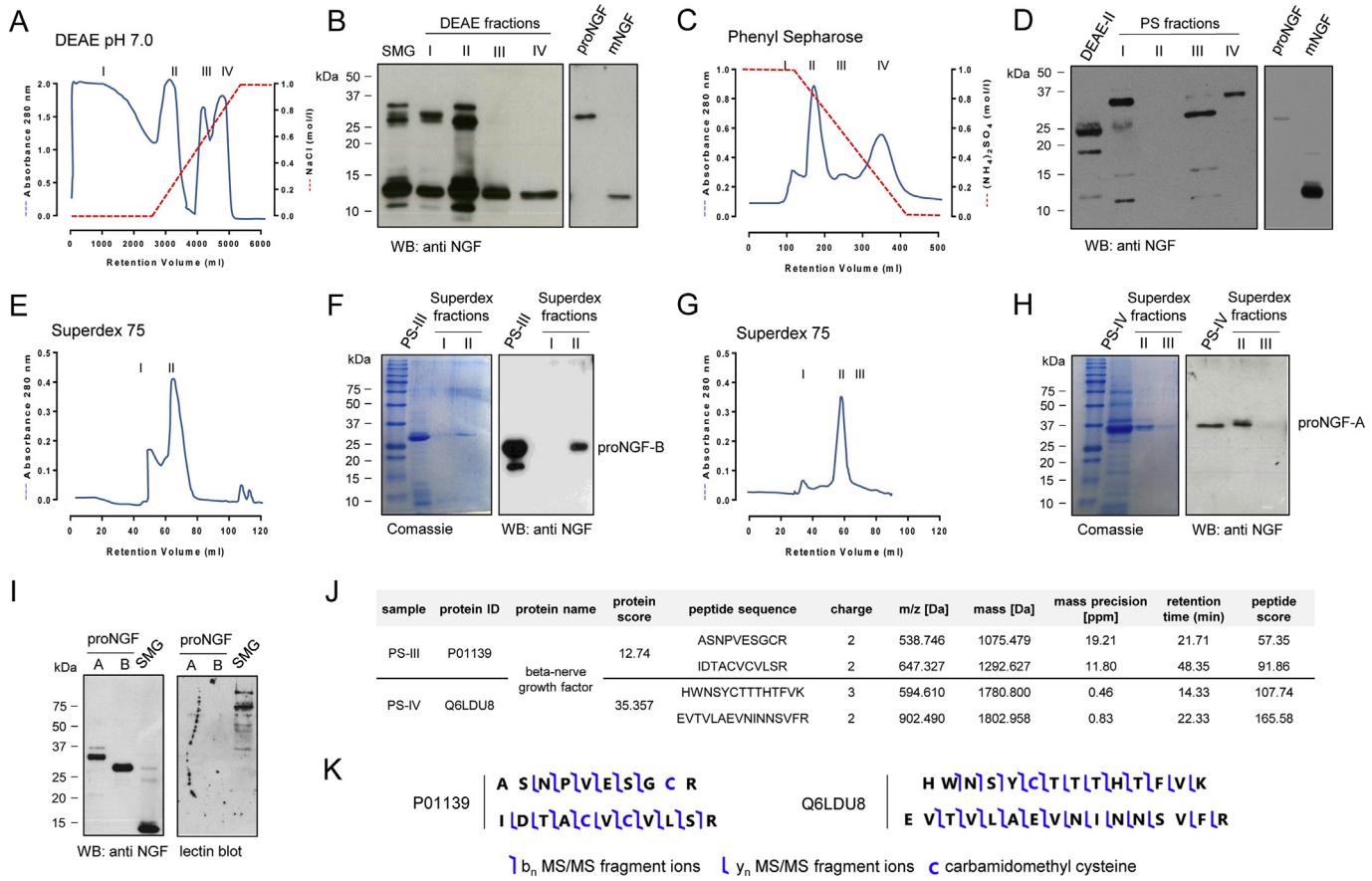

sample	protein ID	protein name	protein score	peptide sequence	charge	m/z [Da]	mass [Da]	mass precision [ppm]	retention time (min)	peptide score
PS-III	P01139	beta-nerve growth factor	12.74	ASNPVESGCR	2	538.746	1075.479	19.21	21.71	57.35
				IDTACVCVLSR	2	647.327	1292.627	11.80	48.35	91.86
PS-IV	Q6LDU8		35.357	HWNSYCTTTHTFVK	3	594.610	1780.800	0.46	14.33	107.74
				EVTVLAEVNINNSVFR	2	902.490	1802.958	0.83	22.33	165.58

Fig. 1. Purification and analysis of native mouse proNGF protein variants. DEAE Sepharose purification chromatogram of mice submaxillary glands extract (A). The dashed line indicates the percentage of NaCl in the elution buffer. Collected fractions were analyzed by Western blot (B). DEAE fraction II (DEAE-II) was purified by Phenyl Sepharose (PS) chromatography (C) and fractions eluted by $(NH_4)_2SO_4$ reverse gradient (dashed line in C) analyzed by Western blot (D). A final purification step by size-exclusion chromatography was performed for PS-III (E) and PS-IV (G) fractions and the eluted fractions were analyzed with Western blot and Coomassie staining (F, H). The purified proNGF-A and proNGF-B, eluted as fraction II in the Superdex 75 chromatography, were also analyzed by comparing anti-NGF Western blot with *Griffonia simplicifolia* type I (GS-I) lectin blotting (I), revealing a lack of glycoside residues linked to the purified proNGFs. (J–K) Information on proteins and peptides identified by nLC-ESI-MS/MS from PS-III and PS-IV fractions after size-exclusion chromatography by Superdex 75 media. The following parameters are reported (J): unique protein sequence identifier (Protein ID) and protein name provided by UniProtKB Database; protein identification Andromeda Score; identified amino acidic peptide sequence; experimental precursor peptide charge and mass/charge in dalton (m/z [Da]); calculated theoretical monoisotopic peptide mass in dalton; calculated peptide mass error in parts per million (mass precision [ppm]); experimental precursor peptide retention time in minutes, and peptide identification Andromeda Score. Sequence annotation sketches of mass spectrometry (K) identified bn and yn ions of proNGF tryptic peptides.

2.4. RNA extraction and real-time PCR analysis

Total RNA, extracted using TRIzol® Reagent (Life Technologies, Rockville, MD, USA), was used for first strand cDNA synthesis (QuantiTect Reverse Transcription Kit, Qiagen, Germany). Real-time PCR was performed on the ABI PRISM™ 7900 HT Sequence Detector platform (Applied Biosystems, Foster City, CA), using Taqman universal Master Mix (Applied Biosystems). TrkA, $p75^{NTR}$, and sortilin expressions were tested using Assays on Demand reagents (TrkA Rn00572130_m1; $p75^{NTR}$ Rn00561634_m1; sortilin Rn01521847_m1; Applied Biosystems). TaqMan® Endogenous Control rat HPRT (Rn01527840_m1; Applied Biosystems) was used as house-keeping gene. Relative quantification was performed using the comparative Ct method and results were expressed in arbitrary units (AU). Expression levels were calculated as $2^{-\Delta Ct}$ (Schmittgen and Livak, 2008).

2.5. ProNgf-A and proNgf-B qPCR design and amplification

To check for the presence of proNgf-A and proNgf-B transcripts in rat PC12 cells and rat tissues, we designed specific qPCR assays, using the Primer-BLAST software available online at http://www.ncbi.nlm.nih.gov/tools/primer-blast/. The primers used to amplify the proNgf-A mRNA spanned from 157 to 285 of the mRNA transcript Ngf-202 (www.ensembl.org/Rattus_norvegicus/Transcript/Summary?db=core;g=ENSRNOG00000016571;r=2:204932159-204940453;t=ENSRNOT00000078376) (Fig. 3B and C; product length 129 bp) while those specific for amplification of the proNgf-B mRNA, transcript Ngf-201(www.ensembl.org/Rattus_norvegicus/Transcript/Summary?db=core;g=ENSRNOG00000016571;r=2:204932159-204940453;t=ENSRNOT00000022200) spanned from 9 to 113 (product length 105 bp). The mean melting temperatures of the primers, listed in Fig. 3C, was 60 °C. All primers showed a GC content of 60–70%, a maximal self-complementarity of 4 nucleotides and a maximal 3′-end complementarity of 0–3 nucleotides. Quantitative PCR of cDNA samples was performed at least in triplicate with a CFX Connect™ Real-Time PCR Detection System (Biorad, California) and the following two-step cycling profile was applied: 30–40 cycles were performed, each with incubation at 95 °C for 15 s followed by 1 min at 60 °C. The cDNA level of β-actin was designed as an internal control. The identity of the PCR products and their purity in each sample were controlled after the last amplification cycle by agarose gel electrophoresis (Fig. 3D). Forward-, internal-reverse- and 3′-UTR-Sanger sequencing analysis was performed by the Sequencing Core Facilities of Eurofins Genomics (Ebersberg, Germany), starting from 70 to 100 ng of template and 10 μM primers

(listed in Fig. 3F). The output data were analyzed by Chromas 2.6.4 tool (https://technelysium.com.au/wp/chromas/, Fig. 3E). To study the identity of the predicted proNgf-A and the new proNgf-A sequence we used the EMBOSS Needle tool (https://www.ebi.ac.uk/Tools/psa/emboss_needle/). The Expasy tool (https://web.expasy.org/translate/) was used to translate the new proNgf-A nucleic acid sequence to the corresponding peptide sequence.

2.6. Cell viability

The potential toxicity of the different mNGF/proNGFs was investigated by cell counting using the Trypan blue exclusion test. For this purpose, cells were seeded in 12-well plates, at a density of 5×10^5 cells/well, and treated with mNGF, proNGF-A or proNGF-B for 24 and/or 48 h. Cell viability was calculated as the number of viable cells divided by the total number of cells within the grids on the haemocytometer.

2.7. Flow cytometry analysis

Samples were acquired on FacsCalibur (BD Biosciences) equipped with a 100 mW argon laser tuned to 488 nm (Ion Laser Technology, Salt Lake City, UT). Emission fluorescence was measured with a DF 530/30 filter for Alexa fluor 488 and a DF 585/42 filter for Alexa fluor 555 and Propidium iodide. The acquired FACS data were analyzed by FlowJo software (FlowJo LLC, Trustees of Leland Stanford Jr. University). All experiments were repeated three times.

2.7.1. Surface immunolabeling

Cells were rinsed in PBS and incubated with the indicated antibodies (Table 1) for 30 min at 4 °C in PBS containing 0.5% BSA. After the cells were washed twice with the above buffer, labeled secondary Abs was added and the mixture was incubated for a further 30 min at 4 °C. The cells were then analyzed on a FACSCalibur.

2.8. Cell differentiation and quantitative morphology

PC12 cells were plated onto 24-well tissue culture plates coated with 20 μg/ml of Poly-L-lysine (P4707 Sigma, St. Louis, MO). Cells were plated at a relatively low density (1×10^4 cells/cm^2) in complete RPMI medium. Two hours after plating, the medium was replaced with serum-free medium supplemented with native mNGF, proNGF-A or proNGF-B. Exposure to serum-free medium alone was used as control. The cells were fed every day by the addition of proNGF/mNGF stimuli. After five days of treatment, morphometric analysis was performed on digitized images of live cells taken under phase contrast illumination with a Motic AE31 trinocular inverted microscope (Motic Asia, Hong Kong). Images of five fields per well were taken and the number of cells that had at least one neurite with a length equal to the cell body diameter was counted using the ImageJ software cell count tool (https://imagej.nih.gov/ij/, NIH, USA) and expressed as a percentage of the total cells in the field. Neurite growth was determined by manually tracing the length of the longest neurite per cell, using the same software, for all cells in a field that had an identifiable neurite and for which the entire neurite arbour could be visualized. Data from the three fields in each well were pooled, and each well was designated as an "n" of one. Experiments were repeated at least three times using cultures prepared on separate days.

2.9. SDS-PAGE and immuno blots

Cells were harvested and lysed with 1% NP-40 (v/v) lysis buffer for 30 min on ice. The protein concentration was measured using Bio-Rad Protein Assay reagent (Bio-Rad, Hercules, CA, USA). Reduced samples were resolved by 8–12% SDS-PAGEand blotted onto nitrocellulose membrane. The primary and HRP-labeled secondary antibodies are reported in Table 1. Blotted membranes were developed with the enhanced chemiluminescence (ECL) detection system (cat. WBKLS0500, Millipore). For lectin blots, membranes were blocked in 0.5% (w/v) casein in T-PBS and incubated for 40 min with 2 μg/ml biotinylated *griffonia simplicifolia* lectin I (GS-I, cat. P0922, Vector Labs, Burlingame, CA) which recognizes glycan residues representative of N-glycosylation in neural cells (Kleene and Schachner, 2004). After washing in T-PBS, membranes were incubated with streptavidin-HRP (cat. SA-5004, Vector Labs) for 30 min. Membranes were washed 3 times for 20 min each with T-PBS prior to developing with ECL substrate.

2.10. Statistical analysis

Statistical analyses were performed using GraphPad Prism 5 (GraphPad Software). Data are presented as mean ± standard error of the mean (SEM). All analyses were two-tailed and P-values < 0.05 were considered statistically significant. P-values were adjusted for multiple comparisons and reported in the figures.

To assess the effect of serum deprivation over time (i.e. proNgf-A and proNgf-B mRNA expression at 4 and 24 h without stimuli) or the effect of mNGF, proNGF-A or proNGF-B, the means were compared by one-way ANOVA and multiple comparisons performed by Bonferroni's post-hoc test.

When the measures for the main variables (effect of different stimuli) were repeated over time (i.e. proNgf-A and proNgf-B mRNA

Table 1
List of used antibodies.

Primary antibody (catalog, manufacture)	Application/Dilution	RRID	Secondary antibody (catalog, manufacture, dilution)
rabbit **anti-TrkA** (ANT-18, Alomone labs)	FACS: 1:200 IF: 1:200	AB_10658910	**Donkey-anti rabbit Alexa-Fluor 555** (A-31572, Thermo Fisher, 1:200) RRID: AB_162543
mouse **anti-p75^{NTR}** (sc-53631, SantaCruz)	CF: 1:200 IF: 1:200	AB_784824	**Donkey-anti mouse Alexa-Fluor 488** (A-21202, Thermo Fisher, 1:200) RRID: AB_141607
rabbit **anti-Sortilin** (PA5-19481, Pierce)	FACS: 1:200 IF: 1:200	AB_10986596	**Donkey-anti rabbit Alexa-Fluor 555** (A-31572, Thermo Fisher, 1:200) RRID: AB_162543
rabbit **anti-NGF M20** (sc-549, SantaCruz)	WB: 1:500	AB_632012	**HRP-conjugated anti-rabbit** (7074, Cell Signaling, 1:4000) RRID: AB_2099233
rabbit **anti-GAPDH** (sc-25778, SantaCruz)	WB: 1:10000	AB_10167668	**HRP-conjugated anti-rabbit** (7074, Cell Signaling, 1:4000) RRID: AB_2099233

IF: immunofluorescence; FACS: Flow cytometry analysis; WB: Western blot.

expression at 4 and 24 h, cell viability at 24 and 48 h), the means were analyzed by two-way ANOVA with family-wise significance level = 0.05. Multiple comparisons using Bonferroni's post-hoc test were then performed according to the main or interaction effects revealed by two-way ANOVA.

A paired *t*-test was performed to compare pairwise the effects of the blockade of TrkA or $p75^{NTR}$ receptor on cell viability and the numbers of neurite-bearing cells within the same experimental group.

An unpaired *t*-test was performed to compare the effects of mNGF and proNGF-A stimuli on neurite elongation in PC12 cells.

3. Results

3.1. Purification and analysis of proNGF protein variants

Two main proNGF protein variants have been found in mouse SMG (Edwards et al., 1986): proNGF-A (molecular weight 34 kDa, UniprotKB: Q6LDU8) and proNGF-B (molecular weight 27 kDa, UniprotKB: P01139) (Bierl et al., 2005; Edwards et al., 1986). We purified both proNGF forms from SMG, by anion exchange, hydrophobic interaction and size exclusion chromatography in sequential steps. Bands corresponding to putative proNGF-A and -B were found mainly in DEAE sepharose fraction II (DEAE-II), eluted at 0.15 M NaCl in anion exchange chromatography (Fig. 1A and B). It is worth noting that both proNGF species bound the DEAE anion exchange medium at pH 7.2, even though their putative isoelectric points should be ≥ 8.0 (Fahnestock et al., 2004a). The behavior of the different proNGFs was well in accord with their putative hydrophobicity, since proNGF-B was eluted in phenyl sepharose medium at a higher concentration of $(NH_4)_2SO_3$ (Fig. 1C and D), than proNGF-A (Fig. 1C and D) which has a 41 aminoacid N-terminal highly hydrophobic tail (Paoletti et al., 2009), lacking in proNGF-B. The final size-exclusion chromatography resulted in satisfactory levels of purity for both the proNGF-A (Fig. 1E and F) and proNGF-B protein variants (Fig. 1G and H). The lectin blot (Fig. 1I) confirmed that the two purified variants are different, unglycosylated NGF-immunoreactive species. Tryptic peptides derived from purified proNGFs were subjected to mass spectrometry analysis and were assigned to amino acid sequences of the beta-nerve growth factor (Fig. 1J and K).

3.2. PC12 cell characterization

To assess the biological effects of the purified proNGF isoforms we used the "gold standard" model for the study of NGF receptor signaling and NGF-mediated responses: the PC12 cell line (Greene and Tischler, 1976). It has been reported that treatment of exponentially growing PC12 with mNGF for 10–14 days (priming) induces the exposure of TrkA receptors on the cell surface (Seeley et al., 1983). We verified these findings by comparing the expression of NGF receptors on unprimed and primed PC12 cells (Fig. S1). We observed that primed PC12 cells showed a higher expression of TrkA, $p75^{NTR}$ and sortilin mRNA (Fig. S1A, right panel) compared with unprimed PC12 (Fig. S1A, left panel). To verify whether these increased expressions corresponded to a consistent exposure of TrkA, $p75^{NTR}$ and sortilin on the cell surface, we performed flow cytometry analysis on live, non-permeabilized cells (Fig. S1B). Flow cytometric profiles of primed PC12 cells, revealed a higher percentage of $TrkA^+$ and $sortilin^+$ cells and a lower percentage of $p75^{NTR+}$ cells (Fig. S1B, lower panels) compared with unprimed PC12 cells (Fig. S1B, upper panels). Confocal microscopy confirmed the relative abundance of $p75^{NTR}$, TrkA and sortilin surface staining in primed cells (Fig. S1C). Thus, since primed PC12 cells are able to respond to both mNGF and proNGFs by activating all of the possible NGF receptors/receptor complexes (Ioannou and Fahnestock, 2017) and since primed PC12 cells are supposed to recapitulate at least some neuronal features (Greene and Tischler, 1976), we decided to perform all subsequent experiments using primed only PC12 cells.

3.3. Basal production and release of proNGF by PC12 cells

To study the effects of purified proNGF protein variants on cell viability and differentiation, we treated PC12 cells with mNGF, proNGF-A or proNGF-B in serum-free media. The dynamics of the persistence of stimuli after their addition to serum-free media were analyzed in time-course experiments (Fig. S2). Exogenous mNGF was detectable for up to 8 h in PC12-conditioned media (Fig. S2A), although a decrease was already evident after 4 h. Both proNGF-A (Fig. S2B) and proNGF-B (Fig. S2C) were still detected in conditioned media up to 24 h after their addition. Of note, bands corresponding to proNGF-A were detected in conditioned media of PC12 cells stimulated with all the mNGF/proNGFs. This indicates a release of endogenous proNGF-A (Figs. S2A–C) that makes it difficult to interpret the persistence dynamics in the media of exogenous proNGF-A (Fig. S2B). Surprisingly, we did not observe any evidence of the previously described conversion of proNGFs into mNGF (Fahnestock et al., 2004b) even though we used native proNGFs that are potentially cleavable by both pro-convertases (Seidah et al., 1996) and metalloproteases (Bruno and Cuello, 2006).

To discriminate between the expression of rat proNgf-A and proNGF-B, we designed two different customized qPCR assays for the selective amplification of the two variants (Fig. 2). We designed forward primers based on the predicted rat proNgf-A and proNgf-B mRNA (Fig. 2A, see section 2.5 for details). The two specific forward primers were then combined with a common reverse primer located outside the spliced region (Fig. 2B and C). The qPCR assays, performed using PC12 cells, rat hippocampal and placenta tissues, were able to amplify both the expected sizes of proNgf-A and proNgf-B cDNA (Fig. 2D), confirming the presence of proNgf-A mRNA in rat cells and tissues. To verify whether the proNgf-A detected in rat tissues was similar to our prediction, we performed a Sanger sequencing (Fig. 2E), using the primers reported in Fig. 2F. Pairwise sequence alignment was 100% identical to the predicted proNgf-A sequence (Fig. S3). The new rat proNgf-A cDNA sequence was deposited in GenBank with accession number: MG721538 (protein_id = "AXN77609"). The same experimental procedures were performed to identify the human proNgf-A variant in CNS and peripheral tissues (Soligo et al. unpublished) and the sequence was deposited in GenBank (accession number: MH358394; protein_id = "AXN77605"). When checked for sequence alignment with the Emboss Needle tool, an 89.6% (275/307) identity and 90.9% (279/307) similarity were found for the mouse proNGF-A (UniprotKB: Q6LDU8) and the peptide sequence derived from the new rat proNgf-A nucleic acid sequence (GenBank record: MG721538; protein_id = "AXN77609") (Figs. S4A–B).

Using the newly designed qPCR assays in time-course experiments, we analyzed proNgf-A and proNgf-B mRNA expression after serum deprivation (Fig. 3A). While proNgf-A mRNA showed a tendency to increase 4 h after serum deprivation (Fig. 3A, left panel), proNgf-B mRNA significantly increased at the late (24 h) time point (Fig. 3A, right panel).

PC12 cells showed a consistent and abundant production of proNGF-A protein, detected in the total lysates, at all time points (Fig. 3B). Indeed, bands corresponding to putative glycosilated-proNGF-A (Soligo et al., 2017), preproNGF-A and unglycosylated proNGF-A, respectively, were detected in total cell lysates, while only the latter seemed to be released in the conditioned media (Fig. 3C). Of note, neither proNGF-B nor mNGF were detected in cell lysates or conditioned media (Fig. 3B and C). Overall, the data shown in Fig. 3 suggest an early adaptive response of the cells based on the production of proNGF-A, while proNGF-B could possibly be involved in a late response (see section 3.4.1).

3.4. Biological effects of proNGF protein variants on PC12 cells

3.4.1. Endogenous ngf gene expression and protein production

We investigated whether treatment with different NGF protein

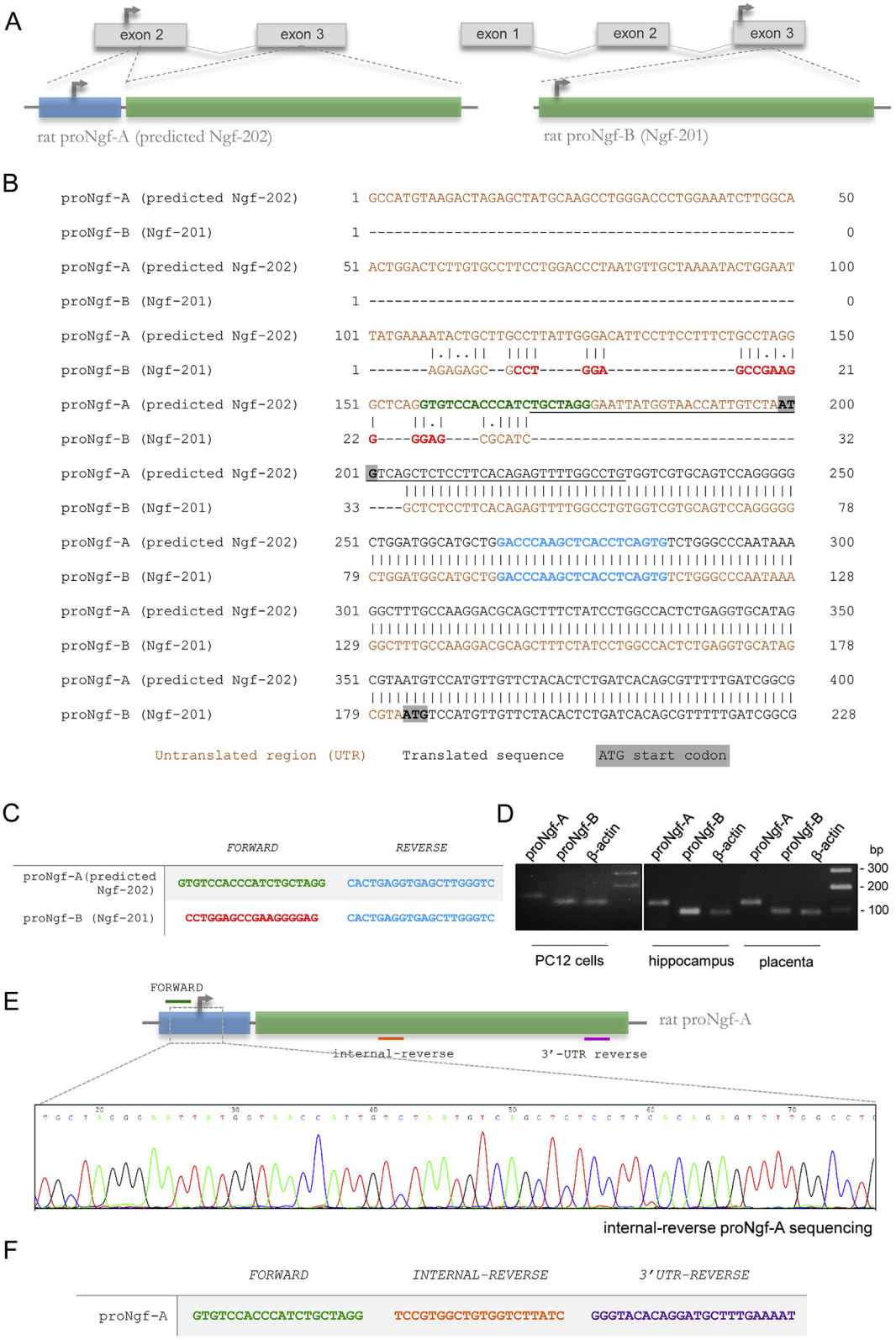

Fig. 2. proNgf mRNA splicing variants were detected in PC12 cells and rat tissues. Two alternate rat proNgf splicing variants have been deposited in public repositories (Ngf-202 and Ngf-201, see section 2.5 for details), the longer one being only predicted. They are depicted in the drawings (A), indicating *ngf* gene exons assembly and mRNAs structure. Alignement of the 5′ regions of the two mRNA variants found in the Ensembl repository were checked (B), revealing differences in the nucleotide sequences in the 5′-UTR. The presence of the predicted proNgf-A and proNgf-B mRNA splicing variants in rat tissues and PC12 cells was detected by setting two different customized qPCR assays for selective amplification of the two variants (B-C). Forward and reverse primers are depicted (C). The rat-derived PC12 cells and rat hippocampal and placenta qPCR products revealed cDNA of both proNgfs, indicating bands of the expected sizes in agarose gel electrophoresis (D). This confirmed the presence of proNgf-A mRNA in rat tissues. Sanger sequencing (E) was performed to verify whether the proNgf-A detected was similar to the predicted form, using the primers reported in panel F. The portion of detected sequence (E), underlined in panel B, represent the partial overlapping of the two mRNA at the 5′-UTR region of proNGF-B.

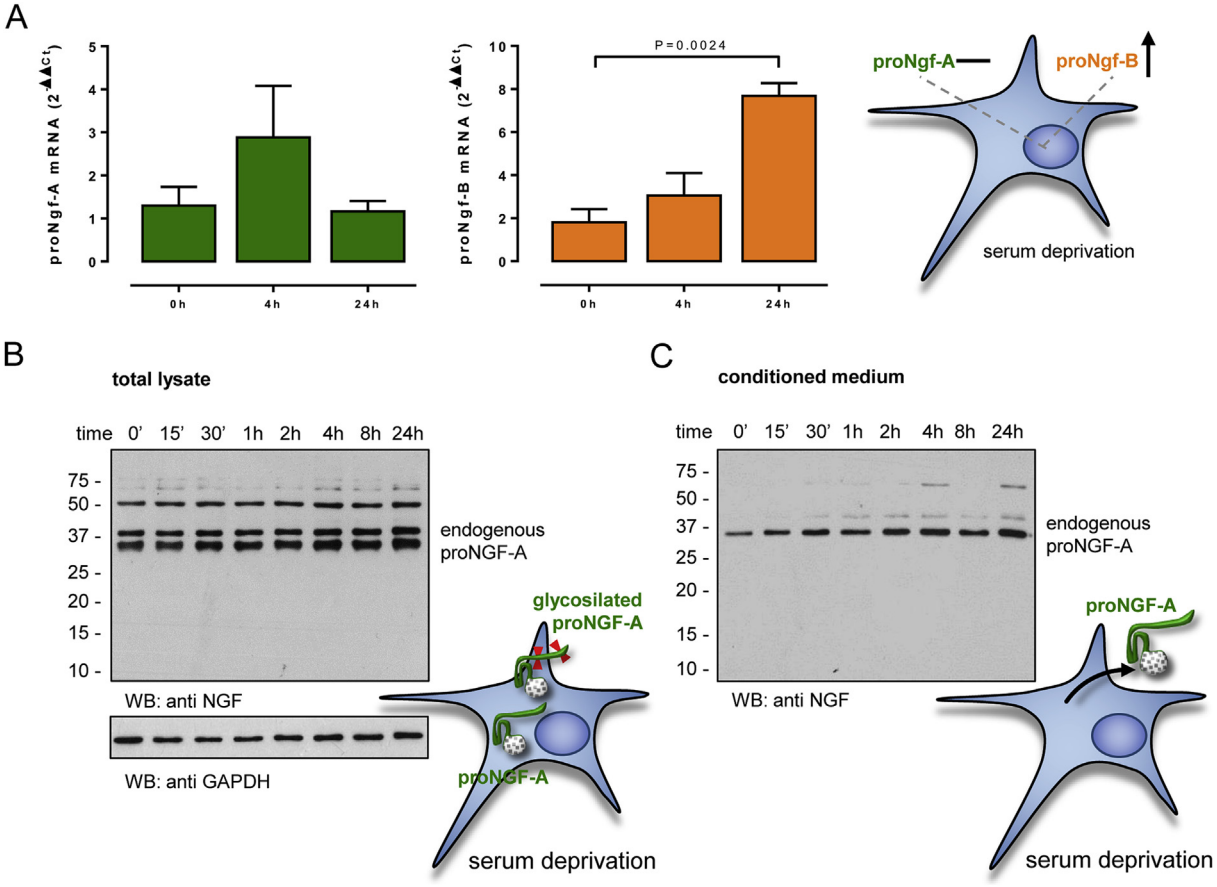

Fig. 3. Expression, intracellular content and release of endogenous proNGF protein variants were modulated by serum starvation. proNgf-A and proNgf-B mRNA expression was measured in serum-deprived primed PC12 cells (A). Only proNgf-B mRNA increased after serum starvation. The drawings on the right side of the panel present a graphical sketch of the modulation of both proNgf mRNAs. Data are presented as mean ± S.E.M. One-way ANOVA was followed by Bonferroni comparison versus unstimulated (US) cells, n = 4, P values are shown in the figure. The intracellular content (B) and the release (C) of endogenous proNGF in serum-deprivation time-course experiments were analyzed by Western blot. The drawings on the right side of each panel represent the location of detected proNGF. Results are representative of three independent experiments.

variants could modulate proNgf-A and proNgf-B gene expression in PC12 cells (Fig. 4A). Only 24 h stimulation with proNGF-B significantly increased proNgf-A mRNA expression, when compared with unstimulated cells (clear columns in the graph) (Fig. 4A, left panel). All NGF protein variants significantly decreased proNgf-B expression 24 h after stimulation, when compared with unstimulated cells (clear columns in the graph) (Fig. 4A, right panel). Overall, these data indicate that different NGF variants may modulate the *ngf* gene transcription and/or mRNA splicing in a selective way and that probably an autocrine regulatory feedback loop could regulate Ngf mRNA expression in PC12 cells.

To correlate mRNA expression and protein production, we analyzed cellular proNGF content after stimulation with mNGF/proNGFs. As hypothesized above, proNGF-B became detectable in cell lysates 48 and 72 h afer serum starvation (Fig. 4B, lanes 1), an effect possibly correlated with the incresed proNgf-B mRNA observed 24 h after serum starvation (Figs. 3A and 4A, right panels). proNGF-B treatmment (Fig. 4B, lanes 3) did not modify the dynamics of proNGF contents observed in untreated cells (Fig. 4B, lanes 1). A consistent production of proNGF-A protein was detected at all time points after stimulation with mNGF (Fig. 4B, lanes 2) and proNGF-A (Fig. 4B, lanes 4). mNGF was never detected, suggesting that in our experimental conditions there is no conversion of PC12-produced proNGF to mNGF.

3.4.2. Cell viability

Cell viability experiments were performed by stimulating serum-deprived PC12 cells with mNGF, proNGF-A and proNGF-B protein variants for 24 and 48 h. As expected, mNGF restored cell viability at both 24 and 48 h, when compared with unstimulated, serum-deprived cells (Fig. 5A). Of note, proNGF-A also restored cell viability after 48 h of serum deprivation, as observed in cells either grown in complete medium or stimulated with mNGF (Fig. 5A). proNGF-B had no effect on serum-deprived PC12 cell viability when compared with unstimulated serum-deprived control cells (Fig. 5A).

The survival effect of proNGF-A treatment could depend on the high expression of TrkA on the cell surface (Fig. S1) and the TrkA/$p75^{NTR}$ balance. To investigate further whether the differential effects of NGF protein variants on cell viability were mediated by their binding to different receptors, we antagonized TrkA or $p75^{NTR}$ receptor before stimulating the cells with mNGF or proNGFs. TrkA-neutralizing chimera (Marsh et al., 2002) consistently decreased the survival of unstimulated mNGF- and proNGF-B-treated PC12 cells but had only a slightly adverse effect on the viability of proNGF-A-treated cells (Fig. 5B). This suggests that receptor(s) other than TrkA may mediate proNGF-A survival effects. Inhibition of $p75^{NTR}$ using the non-peptide LM11A-31 ligand (Massa et al., 2006) significantly increased the viability of both unstimulated and proNGF-B-treated cells (Fig. 5C), suggesting that the decrease in cell viability induced by serum starvation is $p75^{NTR}$-dependent and that proNGF-B does not influence cell viability in these experimental conditions. However, LM11A-31 decreased the survival of proNGF-A-treated cells (Fig. 5C). This suggests that the ability of proNGF-A to prevent cell death induced by serum deprivation

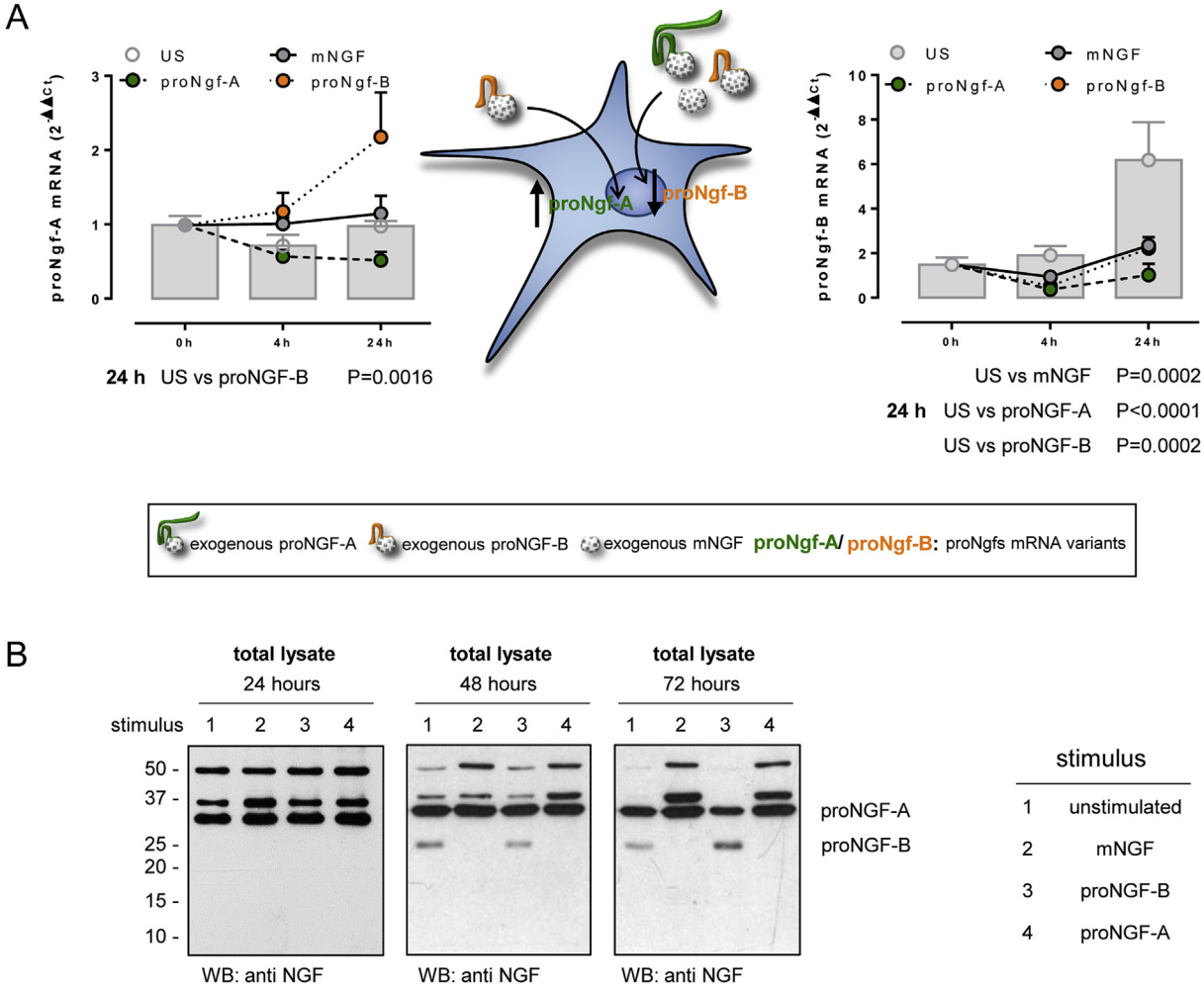

Fig. 4. proNgfs expression and intracellular content were modulated by mNGF/proNGF stimulation. (A) The effects of stimulation with mNGF or proNGF protein variants on proNgf-A (left panel) and proNgf-B (right panel) mRNA expression were analyzed by real time PCR in serum-deprivation time-course experiments. Clear columns in the graphs represent proNgf-A and proNgf-B mRNA in serum-starved, unstimulated cells. The graphic sketch summarizes proNgf-A and proNgf-B mRNA modulation following stimulation with mNGF and proNGF protein variants. Data are presented as mean ± S.E.M. Two-way ANOVA was followed by Bonferroni comparison versus unstimulated (US) cells, n = 4, P values are shown in the figure. (B) Western blot analysis was performed to investigate the time course of proNGF contents in cellular lysate 24 (left panel), 48 (middle panel) and 72 (right panel) hours after stimulation. The presence of a putative proNGF-B protein variant was detected at 48 and 72 h in unstimulated and proNGF-B stimulated cells, together with the progressive disappearance of 50 and 37 kDa bands. Results are representative of three independent experiments.

involves $p75^{NTR}$ receptor activation.

3.4.3. Neurite outgrowth

In order to study the ability of NGF/proNGF protein variants to induce cell differentiation, we stimulated serum-starved PC12 cells for five days with mNGF and proNGFs. Unstimulated PC12 cells were relatively rounded and exhibited retracted cell bodies and processes (Fig. 6A, panel 1). Treatment with both mNGF and proNGF-A resulted in changes in cell body morphology and neurite outgrowth (Fig. 6A, panels 2–3). Treatment with proNGF-B did not, however, elicit any significant effect on PC12 differentiation, since the cells remained round and without any neurite extension (Fig. 6A, panels 4). To quantify PC12 cell differentiation, the number of cells exhibiting neurites (Fig. 6B) and the mean length of neurites (Fig. 6C) were measured. mNGF and proNGF-A induced neurite outgrowth in 55% and 30% of PC12 cells, respectively (Fig. 6B). The lengths of neurites reached means of 748 and 270 μm after treatment with mNGF and proNGF-A, respectively (Fig. 6C). These data suggest that mNGF elicits a more powerful differentiative effect than proNGF-A, which could possibly depend on its higher affinity for the neurotrophic TrkA receptor (Saragovi et al., 1998).

Supporting this hypothesis, the blockade of TrkA completely inhibited neurite outgrowth in cells treated with either mNGF or proNGF-A (Fig. 7A), indicating that TrkA activation is necessary to mediate this specific effect for both protein variants. After $p75^{NTR}$ blockade, stimulation with mNGF or proNGF-A was still effective in inducing cell differentiation (Fig. 7B–D), although to a lesser extent, as suggested by the smaller number of cells bearing neurites (39% and 23%, respectively, Fig. 7C) and by the shorter length of neurites (300 μm and 114 μm, respectively, Fig. 7D), compared with cells not treated with LM11A-31 (Fig. 7C and D, clear columns). Of note, after $p75^{NTR}$ blockade, proNGF-B-treated cells were also able to differentiate, extending neurites from the cell bodies (18% of neurite-bearing cells, Fig. 7C) with a mean length comparable to that measured after proNGF-A treatment (96 μm, Fig. 7D). These data indicate that proNGF-B may have different biological effects depending on the presence of $p75^{NTR}$ and on the TrkA/$p75^{NTR}$ ratio. Thus both the ratio between the different proNGF protein variants and the relative numbers of NGF receptors (Masoudi et al., 2009) are responsible for eliciting distinct responses in PC12 cells.

A

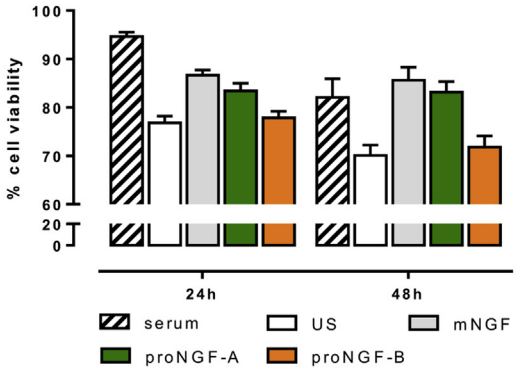

24 hours	
serum vs US	P<0.0001
serum vs proNGF-A	P=0.0077
serum vs proNGF-B	P=0.0001
US vs mNGF	P=0,0229

48 hours	
serum vs US	P=0.0044
serum vs proNGF-B	P=0.0160
US vs mNGF	P=0.0003
US vs proNGF-A	P=0.0020
mNGF vs proNGF-B	P=0.0011
proNGF-A vs proNGF-B	P=0.0070

B **TrkA chimera**

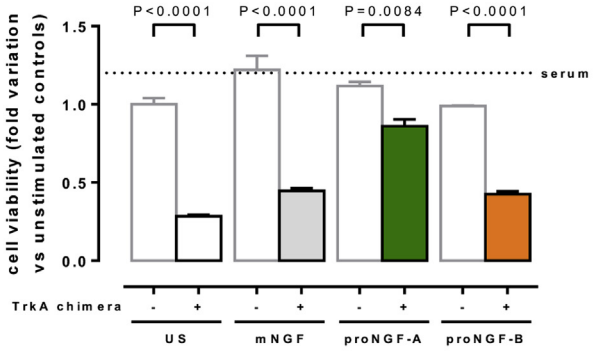

comparison between TrkA chimera-treated cells

US vs mNGF	P=0.0688	ns
US vs proNGF-A	P=0.0006	***
US vs proNGF-B	P=0.1118	ns
mNGF vs proNGF-A	P=0.0022	**
mNGF vs proNGF-B	P>0.9999	ns
proNGF-A vs proNGF-B	P=0.0018	**

C **p75^{NTR} LM11A-31**

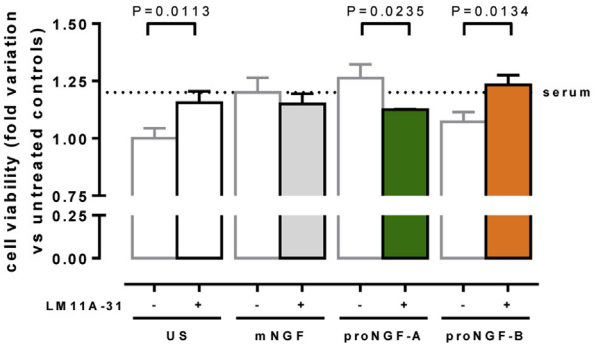

comparison between p75^{NTR} LM11A-31-treated cells

US vs mNGF	P>0.9999	ns
US vs proNGF-A	P=0.5093	ns
US vs proNGF-B	P=0.1707	ns
mNGF vs proNGF-A	P=0.6624	ns
mNGF vs proNGF-B	P=0.2074	ns
proNGF-A vs proNGF-B	P>0.9999	ns

Fig. 5. Cell viability in primed PC12 cells after exposure to mNGF and proNGF protein variants. Cell viability, measured as the percentage of viable cells in total PC12 cells, was measured 24 and 48 h after serum starvation and exposure to mNGF or proNGF protein variants (A). The striped columns represent the percentage of cell viability of PC12 cells grown with serum. The table (A, right panel) reports the comparisons reaching statistical significance within any time point. (B–C) The effects of TrkA or p75^{NTR}blockade, by TrkA chimera and non-peptide LM11A-31 ligand respectively, on PC12 cell viability were measured 48 h after serum starvation or stimulation with mNGF and proNGFs. The data are expressed as cell viability fold variations in unstimulated cells not pre-treated with TrkA chimera or LM11A-31 ligand (first column on the left side of panels B–C). The graphs show the intra-group P values (TrkA chimera or LM11A-31 ligand, comparison of untreated versus treated groups) and the tables (right side of panels B and C) show the inter-group P values (comparison between different stimulations after pretreatment with TrkA chimera or LM11A-31). The dotted lines in the graphs in panels B and C indicate the cell viability values of untreated PC12 cells grown in the presence of serum. Data are presented as mean ± S.E.M. (A) Two-way ANOVA was followed by Bonferroni multiple comparison. (B–C) Paired *t*-test for comparisons of TrkA chimera or non-peptide LM11A-31 ligand effects (P values in the graphs) and One-Way ANOVA followed by Bonferroni multiple comparison for the effects of different stimuli on TrkA chimera- or non-peptide LM11A-31 ligand -treated cells (P values in the tables). n = 3, P values are shown in the figure.

4. Discussion

ProNGF is the predominant form of NGF detectable in human (Fahnestock et al., 2001) and rodent (Bierl et al., 2005; Protto et al., 2019; Soligo et al., 2015) brains and its protein levels increase in human neurodegenerative diseases (Fahnestock et al., 2001; Iulita and Cuello, 2014) and some tumor types (reviewed in Bradshaw et al., 2015). In vitro studies have shown that proNGF can be either

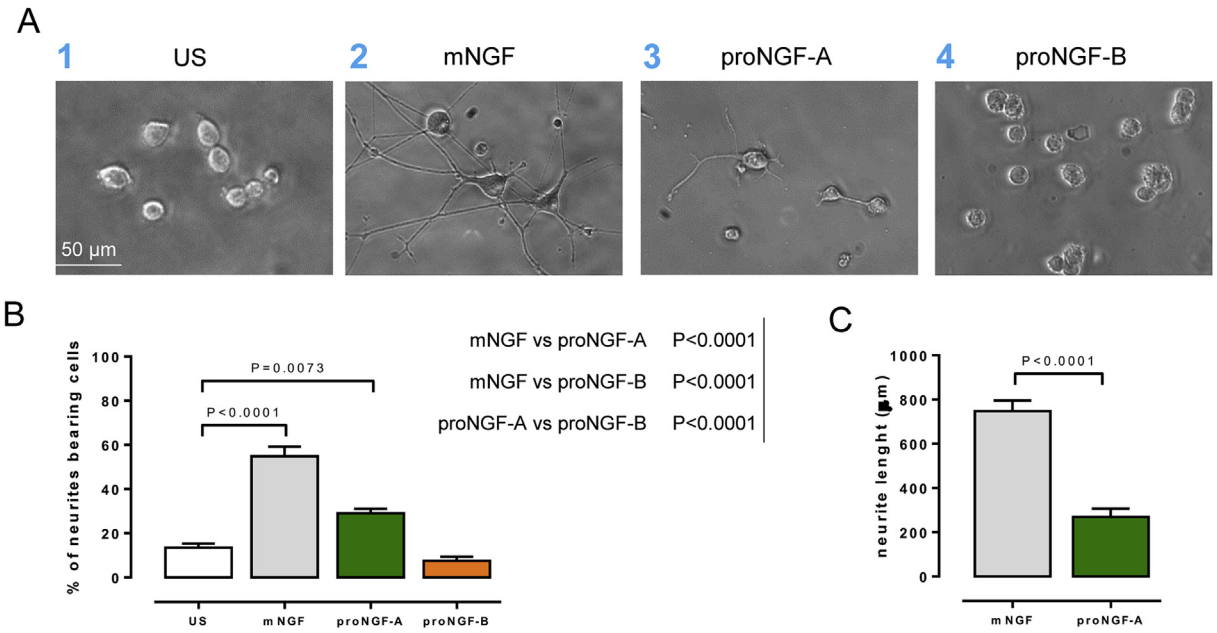

Fig. 6. Cell differentiation in primed PC12 cells after exposure to mNGF and proNGF. The effects of different stimuli on cell differentiation were analyzed in primed PC12 cells treated with mNGF and proNGFs for five days. (A) Representative images of unstimulated (US, panel 1), mNGF- (panel 2), proNGF-A- (panel 3) and proNGF-B-treated (panel 4) cells. Scale bar: 50 µm. (B) The number of cells that had at least one neurite with a length equal to the cell body diameter was reported and expressed as a percentage of the total cells in the field (five fields were analyzed and the data pooled in each experiment). The P values in the graph refer to the comparison versus unstimulated (US) cells. The table (right side of panel B) shows the P values of the comparison among all the other groups. (C) Neurite growth was determined by manually tracing the length of the longest neurite per cell for all cells in a field that had an identifiable neurite (three fields were analyzed and the data pooled in each experiment). Experiments were repeated at least three times using cultures prepared on separate days. Data are presented as mean ± S.E.M. For percentages of neurite-bearing cells (B): one-way ANOVA was followed by Bonferroni multiple comparison, n = 3, P values are shown in the figure. For neurite length comparison (C): Unpaired *t*-test, n = 3 (see section 2.8 for details).

neurotoxic (Lee et al., 2001; Nykjaer et al., 2004) or neurotrophic (Fahnestock et al., 2004b; Rattenholl et al., 2001), depending on the balance between the different NGF receptors (Ioannou and Fahnestock, 2017; Masoudi et al., 2009) and may also have a role in lymphnode invasion and tumor metastases (Demont et al., 2012). Although the existence of several proNgf mRNA species, derived from alternative splicing (Edwards et al., 1986) and/or activation of different promoters (Racke et al., 1996), has been described since the end of the 1980s', the possible peculiar biological activity of the diverse proNGF forms is still unknown. In the present work, we pursued a first analysis of the possible specific biological role of the two main proNGF variants using the PC12 cellular model (Greene, 1978; Greene and Tischler, 1976).

We found that proNGF-B was unable to exert pro-survival and neurotrophic actions when all components of the proNGF/NGF receptor complexes, TrkA, $p75^{NTR}$ and sortilin, are present on the cell surface. However, proNGF-A was able to protect PC12 cells from cellular stress and death induced by serum starvation in a $p75^{NTR}$- and/or TrkA-dependent manner. proNGF-A also induced neuronal differentiation of PC12 cells, though with less potency than did mNGF. Our data also demonstrated for the first time that the PC12 rat-derived cell line and rat tissues do express the proNgf-A transcript, a finding that had previously only been predicted by computational analysis of the genomic sequences (see section 2.5 for links to sequences) and protein primary structure inferred from homology (http://www.uniprot.org/uniprot/A0A0G2K2Z7).

To distinguish between the possible different effects of proNGF-A and proNGF-B, we used proNGF isoforms purified from mouse submaxillary glands. Since obtaining a functional, well-formed protein is a major problem in protein expression experiments (Edwards et al., 1988), we purified proNGFs from tissues with the aim of using native proteins as stimuli for PC12 cells in a more physiological approach, rather than stimulating the cells with recombinant proteins obtained using protein expression prokaryotic/eukaryotic vectors, widely used in functional studies (Arisi et al., 2014; D'Onofrio et al., 2011; Ioannou and Fahnestock, 2017; Masoudi et al., 2009). The major challenge in purifying native mouse proNGF was related to its negative molecular net charge, different from what expected (Fahnestock et al., 2004a) and probably due to its association with acidic proteins, similarly to what has been reported for mNGF (Shooter, 2001). In accordance with previous reports (Fahnestock et al., 2004a), we found that the proNGF was resolved as a dimer in the final chromatographic step, a size-exclusion chromatography in the presence of urea. The final control step, performed by mass spectrometry, confirmed the identity of the purified proNGFs and the successful elimitation of contaminants, such as kallikrein or renin, which are known to strongly interact with NGF, purified from mice SMG (Cozzari et al., 1973; Shooter, 2001). The behaviour of the two proteins in the hydrophobic interaction-based chromatography and the analysis of protein glycosilation also excluded the possibility that the two purified products correspond to the same protein with different glycosylation moieties.

An initial clue regarding the possible different physiological roles of the two proNGF forms was suggested by their endogenous expression by PC12 cells. We observed an increase in proNgf-B mRNA, starting 24 h after serum starvation that could be correlated with the production of proNGF-B protein observed at 48 and 72 h. On the other hand, proNgf-A mRNA showed only an early (4 h after starvation) tendency to increase, while the protein levels were found consistently and abundantly present throughout the course of the experiment. It is probable that our newly designed qPCR assays have different sensitivities, making it difficult to determine the relative abundance of the two transcripts. Nevertheless, our protein data point to proNGF-A as the main Ngf transcript expressed in PC12 cells, similar to what has been previously observed in mouse (Bierl et al., 2005) and rat brain tissues (Protto et al., 2019; Soligo et al., 2015).

The finding that stimulation with mNGF/proNGF protein variants may differentially affect the expression of the two proNgf transcripts,

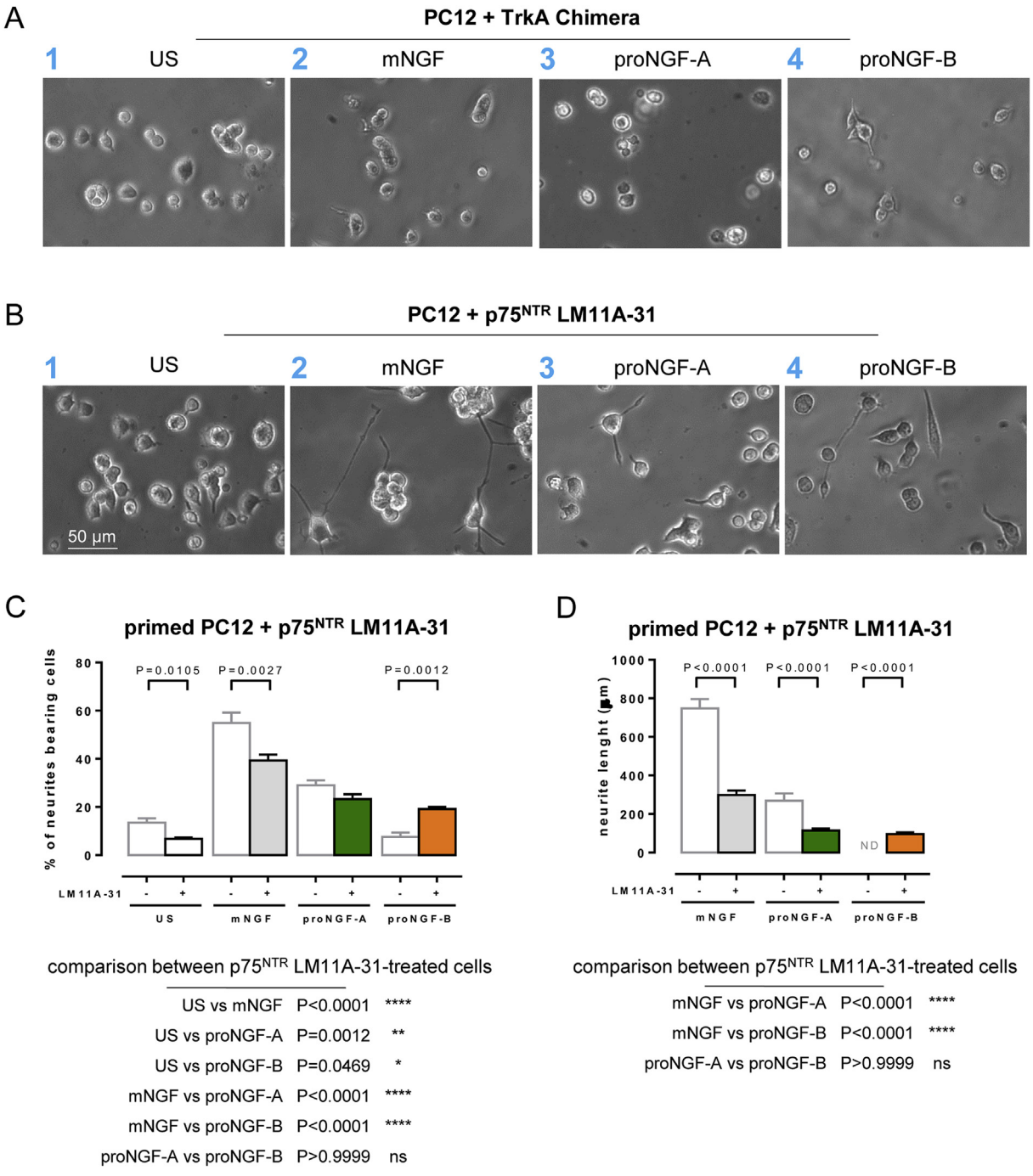

comparison between p75NTR LM11A-31-treated cells

US vs mNGF	P<0.0001	****
US vs proNGF-A	P=0.0012	**
US vs proNGF-B	P=0.0469	*
mNGF vs proNGF-A	P<0.0001	****
mNGF vs proNGF-B	P<0.0001	****
proNGF-A vs proNGF-B	P>0.9999	ns

comparison between p75NTR LM11A-31-treated cells

mNGF vs proNGF-A	P<0.0001	****
mNGF vs proNGF-B	P<0.0001	****
proNGF-A vs proNGF-B	P>0.9999	ns

Fig. 7. TrkA or p75NTR blockade differently affected the action of mNGF and proNGF on PC12 cell differentiation. The effects of TrkA or p75NTR blockade on cell differentiation were measured in primed PC12 cells. Representative images of unstimulated (US, panel 1), mNGF- (panel 2), proNGF-A- (panel 3) and proNGF-B-treated (panel 4) cells in the presence of TrkA chimera (A) or non-peptide LM11A-31 (B). Scale bar: 50 µm. No neurite extension from the cell bodies was observed after pre-treatment with TrkA chimera in any experimental groups. (C) The percentage of neurite-bearing cells treated or not with the non-peptide LM11A-31 ligand is reported and expressed as a percentage of the total cells in the field (five fields were analyzed and the data pooled in each experiment). The P values reported in the graph refer to the pairwise comparison between LM11A-31-treated and untreated cells. The table (C, below the graph) shows P values of the multiple comparison between all the LM11A-31-treated groups. (D) The neurite lengths of PC12 cells treated with mNGF, proNGF-A and proNGF-B are reported (three fields were analyzed and the data pooled in each experiment). The P values in the graph refer to the pairwise comparison between LM11A-31-treated and untreated cells. The table (D, below the graph) shows P values of the comparison between all the LM11A-31-treated groups. Experiments were repeated at least three times using cultures prepared on separate days. Data are presented as mean ± S.E.M. n = 3. For comparison between LM11A-31-treated and -untreated cells: paired *t*-test, P values are shown in the graphs. For comparison of the effects of different stimuli on LM11A-31-treated cells: one-Way ANOVA was followed by Bonferroni multiple comparison, P values are reported in the tables below the graphs.

with a prevalent down-regulation of proNgf-B and up-regulation of proNgf-A, and the production of proNGF proteins, suggests that an autocrine feedback loop may regulate the action of mNGF/proNGFs in PC12 cells, in a manner similar to what observed in other tumor cells (Dolle et al., 2003). In view of the described neurotoxic activity of proNGF-B (Lee et al., 2001; Nykjaer et al., 2004) and taking into account the present findings regarding a neurotrophic action of proNGF-A, our data could be interpreted as an attempt by the cells to activate a

proNGF-A-based, autocrine, protective mechanism. However, at 48 h after proNGF-B stimulation, PC12 cells also produced proNGF-B. This could reflect the failure of cells to balance the physiological relative ratio of the two proNGF proteins, which could be the result of a late and massive production of proNgf-B as well as of the intracellular processing of high molecular weight intermediates, as suggested by the disappearance of some of the high molecular weight isoforms of proNGF in both serum-deprived and proNGF-B-treated cells, at 48–72 h (Fig. 4B).

We observed that both mNGF and proNGF-A can support cell survival and stimulate neurite outgrowth in serum-starved PC12 cells. This is in agreement with previous reports indicating a neurotrophic effect of cleavage-resistant recombinant proNGF (Ioannou and Fahnestock, 2017; Masoudi et al., 2009). Since proNGF undergoes intra- and/or extra-cellular cleavage to generate mNGF (Bruno and Cuello, 2006; Seidah et al., 1996), it is conceivable that the neurotrophic effects that we observed after native proNGF stimulation may depend on the action of mNGF. However, this hypothesis contrasts with previous reports (Masoudi et al., 2009) and with our present observations, indicating a specific neurotrophic action of proNGF. In our experiments, native, potentially cleavable, proNGF-A and proNGF-B, as well as mNGF, were shown to exert distinct actions on PC12 cells, and their activity depended on different receptors/receptor complexes. We found no mNGF in cell lysates and in conditioned media, neither in basal conditions nor after proNGF supplementation. This is supported by previous reports indicating that the only NGF protein detectable in mouse (Bierl et al., 2005), rat (Soligo et al., 2015) and human (Fahnestock et al., 2001) brains, in both physological and pathological conditions, is proNGF. Furthermore, proNGF seems to be less prone to degradation by extracelluar proteases, as suggested by our data on the different dynamics of stimuli persistence in the culture media, Thus, overall, our findings clearly indicate that the activity of the proneurotrophin may be mainly or totally ascribed to proNGF rather than mNGF.

Our data indicate that native mouse proNGF-B was able neither to exert pro-apoptotic effects nor to stimulate survival/differentiation unless $p75^{NTR}$ was antagonized. It is worth noting that the first identification of the selective pro-apoptotic challenge of proNGF to the $p75^{NTR}$-sortilin complex (Nykjaer et al., 2004) was performed using recombinant mouse (241 aminoacid-long) proNGF-B (Rattenholl et al., 2001). Since we demonstrated that primed PC12 cells display a receptor phenotype that ensures a potential responsivity to all the different proNGF/NGF forms, it is conceivable that proNGF-B could challenge the $p75^{NTR}$-sortilin complex in our experimental setting. Although further characterization of the observed absence of the expected pro-apoptotic effect is needed, it should be borne in mind that proNGF-A was consistently released by PC12 cells, even after stimulation with proNGF-B (Fig. S2), thus possibly counteracting the neurotoxic effects of proNGF-B (Nykjaer et al., 2004). On the other hand, proNGF-A exerted a pro-survival effect, even after the neutralization of TrkA, suggesting its potential ability to activate the described $p75^{NTR}$-mediated, TrkA independent pro-survival signaling pathway (Howard et al., 2013). Overall our data indicate that while proNGF-B may challenge TrkA, though possibly retaining a preferential binding to the $p75^{NTR}$-sortilin complex (Nykjaer et al., 2004), some of the effects of proNGF-A may not necessarily rely on the presence of TrkA.

In our present study we used the PC12 cell line, which is considered the gold standard for assessing the biological activity of NGF *in vitro* (Greene, 1978; Masoudi et al., 2009; Rudkin et al., 1989). However, the potential translational implications of our work call for a more exhaustive characterization of the effects of different NGFs in other cells and tissue models, such as those represented by primary neuronal cells, isolated sensory or sympathetic ganglia and other cancer cell lines. Although this represents a possible limitation of the present study, the preliminary results of our ongoing *in vivo* experiments indicate that exogenous proNGF-A exerts a pro-survival and pro-neurotrophic activity on granular neurons of the hippocampal dentate gyrus, in a rat model of neurodegeneration (Soligo, manuscript in preparation). This indicates the need to investigate futrther the pharmacology of proNGF-A, in order to gain deeper knowledge of its efficacy and safety profile in comparison with that of mNGF (Aloe et al., 2012). Moreover, a better understanding of the physiological and pathological roles of the two proNGF variants could be useful for their possible clinical application as biomarkers to monitor the development and progression of neural damage secondary to neurotraumas and neurodegenerative diseases as well as the potential tumorigenesis and metastatic potential of several tumor types (Bradshaw et al., 2015; Demont et al., 2012; Truzzi et al., 2008)

5. Conclusion

In conclusion, our data indicate that the development and progression of neurodegenerative and cancer diseases may be affected not only by the ratio between mature and proNGF (Capsoni et al., 2011; Soligo et al., 2015; Tiveron et al., 2013) and the relative expression levels of different NGF receptors (Ioannou and Fahnestock, 2017; Masoudi et al., 2009), but also by the relative expression levels of different proNgf transcripts, their regulation at transcription and mRNA splicing levels (Edwards et al., 1986; Racke et al., 1996; West et al., 2014), and the possible related imbalance of their derived protein variants and its deviation from physiological equilibrium.

Declarations of interest

The Authors declare they have no conflicts of interest.

Funding

This research did not receive any specific grant from funding agencies in the public, commercial or not-for-profit sectors.

Acknowledgements

The authors thank Prof. Silvia Biocca (Department of Systems Medicine, University of Rome Tor Vergata) for the generous gift of PC12 cells.

We thank Mrs Margaret Wayne Starace for English language editing.

Appendix A. Supplementary data

Supplementary data to this article can be found online at https://doi.org/10.1016/j.neuint.2019.104498.

References

Aloe, L., Rocco, M.L., Bianchi, P., Manni, L., 2012. Nerve growth factor: from the early discoveries to the potential clinical use. J. Transl. Med. 10, 239.

Arisi, I., D'Onofrio, M., Brandi, R., Malerba, F., Paoletti, F., Storti, A.E., Florenzano, F., Fasulo, L., Cattaneo, A., 2014. proNGF/NGF mixtures induce gene expression changes in PC12 cells that neither singly produces. BMC Neurosci. 15, 48.

Beattie, M.S., Harrington, A.W., Lee, R., Kim, J.Y., Boyce, S.L., Longo, F.M., Bresnahan, J.C., Hempstead, B.L., Yoon, S.O., 2002. ProNGF induces p75-mediated death of oligodendrocytes following spinal cord injury. Neuron 36, 375–386.

Bierl, M.A., Jones, E.E., Crutcher, K.A., Isaacson, L.G., 2005. 'Mature' nerve growth factor is a minor species in most peripheral tissues. Neurosci. Lett. 380, 133–137.

Bradshaw, R.A., Pundavela, J., Biarc, J., Chalkley, R.J., Burlingame, A.L., Hondermarck, H., 2015. NGF and ProNGF: regulation of neuronal and neoplastic responses through receptor signaling. Adv Biol Regul 58, 16–27.

Bruno, M.A., Cuello, A.C., 2006. Activity-dependent release of precursor nerve growth factor, conversion to mature nerve growth factor, and its degradation by a protease cascade. Proc. Natl. Acad. Sci. U. S. A. 103, 6735–6740.

Capsoni, S., Brandi, R., Arisi, I., D'Onofrio, M., Cattaneo, A., 2011. A dual mechanism linking NGF/proNGF imbalance and early inflammation to Alzheimer's disease neurodegeneration in the AD11 anti-NGF mouse model. CNS Neurol. Disord. - Drug Targets 10, 635–647.

Capsoni, S., Cattaneo, A., 2006. On the molecular basis linking Nerve Growth Factor (NGF) to Alzheimer's disease. Cell. Mol. Neurobiol. 26, 619–633.

Chao, M.V., Rajagopal, R., Lee, F.S., 2006. Neurotrophin signalling in health and disease. Clin. Sci. (Lond.) 110, 167–173.

Chiaretti, A., Conti, G., Falsini, B., Buonsenso, D., Crasti, M., Manni, L., Soligo, M., Fantacci, C., Genovese, O., Calcagni, M.L., Di Giuda, D., Mattoli, M.V., Cocciolillo, F., Ferrara, P., Ruggiero, A., Staccioli, S., Colafati, G.S., Riccardi, R., 2017. Intranasal Nerve Growth Factor administration improves cerebral functions in a child with severe traumatic brain injury: a case report. Brain Inj. 31, 1538–1547.

Cozzari, C., Angeletti, P.U., Lazar, J., Orth, H., Gross, F., 1973. Separation of isorenin activity from nerve growth factor (NGF) activity in mouse submaxillary gland extracts. Biochem. Pharmacol. 22, 1321–1327.

Cuello, A.C., Bruno, M.A., 2007. The failure in NGF maturation and its increased degradation as the probable cause for the vulnerability of cholinergic neurons in Alzheimer's disease. Neurochem. Res. 32, 1041–1045.

Cuello, A.C., Bruno, M.A., Allard, S., Leon, W., Iulita, M.F., 2010. Cholinergic involvement in Alzheimer's disease. A link with NGF maturation and degradation. J. Mol. Neurosci. 40, 230–235.

D'Onofrio, M., Paoletti, F., Arisi, I., Brandi, R., Malerba, F., Fasulo, L., Cattaneo, A., 2011. NGF and proNGF regulate functionally distinct mRNAs in PC12 cells: an early gene expression profiling. PLoS One 6 e20839.

Demont, Y., Corbet, C., Page, A., Ataman-Onal, Y., Choquet-Kastylevsky, G., Fliniaux, I., Le Bourhis, X., Toillon, R.A., Bradshaw, R.A., Hondermarck, H., 2012. Pro-nerve growth factor induces autocrine stimulation of breast cancer cell invasion through tropomyosin-related kinase A (TrkA) and sortilin protein. J. Biol. Chem. 287, 1923–1931.

Dolle, L., El Yazidi-Belkoura, I., Adriaenssens, E., Nurcombe, V., Hondermarck, H., 2003. Nerve growth factor overexpression and autocrine loop in breast cancer cells. Oncogene 22, 5592–5601.

Edwards, R.H., Selby, M.J., Mobley, W.C., Weinrich, S.L., Hruby, D.E., Rutter, W.J., 1988. Processing and secretion of nerve growth factor: expression in mammalian cells with a vaccinia virus vector. Mol. Cell. Biol. 8, 2456–2464.

Edwards, R.H., Selby, M.J., Rutter, W.J., 1986. Differential RNA splicing predicts two distinct nerve growth factor precursors. Nature 319, 784–787.

Fahnestock, M., Michalski, B., Xu, B., Coughlin, M.D., 2001. The precursor pro-nerve growth factor is the predominant form of nerve growth factor in brain and is increased in Alzheimer's disease. Mol. Cell. Neurosci. 18, 210–220.

Fahnestock, M., Yu, G., Coughlin, M.D., 2004a. ProNGF: a neurotrophic or an apoptotic molecule? Prog. Brain Res. 146, 101–110.

Fahnestock, M., Yu, G., Michalski, B., Mathew, S., Colquhoun, A., Ross, G.M., Coughlin, M.D., 2004b. The nerve growth factor precursor proNGF exhibits neurotrophic activity but is less active than mature nerve growth factor. J. Neurochem. 89, 581–592.

Greene, L.A., 1978. Nerve growth factor prevents the death and stimulates the neuronal differentiation of clonal PC12 pheochromocytoma cells in serum-free medium. J. Cell Biol. 78, 747–755.

Greene, L.A., Tischler, A.S., 1976. Establishment of a noradrenergic clonal line of rat adrenal pheochromocytoma cells which respond to nerve growth factor. Proc. Natl. Acad. Sci. U. S. A. 73, 2424–2428.

Harrington, A.W., Leiner, B., Blechschmitt, C., Arevalo, J.C., Lee, R., Morl, K., Meyer, M., Hempstead, B.L., Yoon, S.O., Giehl, K.M., 2004. Secreted proNGF is a pathophysiological death-inducing ligand after adult CNS injury. Proc. Natl. Acad. Sci. U. S. A. 101, 6226–6230.

Hempstead, B.L., 2014. Deciphering proneurotrophin actions. Handb. Exp. Pharmacol. 220, 17–32.

Howard, L., Wyatt, S., Nagappan, G., Davies, A.M., 2013. ProNGF promotes neurite growth from a subset of NGF-dependent neurons by a p75NTR-dependent mechanism. Development 140, 2108–2117.

Ioannou, M.S., Fahnestock, M., 2017. ProNGF, but not NGF, switches from neurotrophic to apoptotic activity in response to reductions in TrkA receptor levels. Int. J. Mol. Sci. 18.

Iulita, M.F., Cuello, A.C., 2014. Nerve growth factor metabolic dysfunction in Alzheimer's disease and Down syndrome. Trends Pharmacol. Sci. 35, 338–348.

Kleene, R., Schachner, M., 2004. Glycans and neural cell interactions. Nat. Rev. Neurosci. 5, 195–208.

Lee, R., Kermani, P., Teng, K.K., Hempstead, B.L., 2001. Regulation of cell survival by secreted proneurotrophins. Science 294, 1945–1948.

Marsh, D.R., Wong, S.T., Meakin, S.O., MacDonald, J.I., Hamilton, E.F., Weaver, L.C., 2002. Neutralizing intraspinal nerve growth factor with a trkA-IgG fusion protein blocks the development of autonomic dysreflexia in a clip-compression model of spinal cord injury. J. Neurotrauma 19, 1531–1541.

Masoudi, R., Ioannou, M.S., Coughlin, M.D., Pagadala, P., Neet, K.E., Clewes, O., Allen, S.J., Dawbarn, D., Fahnestock, M., 2009. Biological activity of nerve growth factor precursor is dependent upon relative levels of its receptors. J. Biol. Chem. 284, 18424–18433.

Massa, S.M., Xie, Y., Yang, T., Harrington, A.W., Kim, M.L., Yoon, S.O., Kraemer, R., Moore, L.A., Hempstead, B.L., Longo, F.M., 2006. Small, nonpeptide p75NTR ligands induce survival signaling and inhibit proNGF-induced death. J. Neurosci. 26, 5288–5300.

Nykjaer, A., Lee, R., Teng, K.K., Jansen, P., Madsen, P., Nielsen, M.S., Jacobsen, C., Kliemannel, M., Schwarz, E., Willnow, T.E., Hempstead, B.L., Petersen, C.M., 2004. Sortilin is essential for proNGF-induced neuronal cell death. Nature 427, 843–848.

Paoletti, F., Covaceuszach, S., Konarev, P.V., Gonfloni, S., Malerba, F., Schwarz, E., Svergun, D.I., Cattaneo, A., Lamba, D., 2009. Intrinsic structural disorder of mouse proNGF. Proteins 75, 990–1009.

Protto, V., Soligo, M., De Stefano, M.E., Farioli-Vecchioli, S., Marlier, L., Nistico, R., Manni, L., 2019. Electroacupuncture in Rats Normalizes the Diabetes-Induced Alterations in the Septo-Hippocampal Cholinergic System. Hippocampus.

Racke, M.M., Mason, P.J., Johnson, M.P., Brankamp, R.G., Linnik, M.D., 1996. Demonstration of a second pharmacologically active promoter region in the NGF gene that induces transcription at exon 3. Brain Res Mol Brain Res 41, 192–199.

Rappsilber, J., Mann, M., Ishihama, Y., 2007. Protocol for micro-purification, enrichment, pre-fractionation and storage of peptides for proteomics using StageTips. Nat. Protoc. 2, 1896–1906.

Rattenholl, A., Lilie, H., Grossmann, A., Stern, A., Schwarz, E., Rudolph, R., 2001. The pro-sequence facilitates folding of human nerve growth factor from Escherichia coli inclusion bodies. Eur. J. Biochem. 268, 3296–3303.

Rudkin, B.B., Lazarovici, P., Levi, B.Z., Abe, Y., Fujita, K., Guroff, G., 1989. Cell cycle-specific action of nerve growth factor in PC12 cells: differentiation without proliferation. EMBO J. 8, 3319–3325.

Saragovi, H.U., Zheng, W., Maliartchouk, S., DiGugliemo, G.M., Mawal, Y.R., Kamen, A., Woo, S.B., Cuello, A.C., Debeir, T., Neet, K.E., 1998. A TrkA-selective, fast internalizing nerve growth factor-antibody complex induces trophic but not neuritogenic signals. J. Biol. Chem. 273, 34933–34940.

Schmittgen, T.D., Livak, K.J., 2008. Analyzing real-time PCR data by the comparative C(T) method. Nat. Protoc. 3, 1101–1108.

Seeley, P.J., Keith, C.H., Shelanski, M.L., Greene, L.A., 1983. Pressure microinjection of nerve growth factor and anti-nerve growth factor into the nucleus and cytoplasm: lack of effects on neurite outgrowth from pheochromocytoma cells. J. Neurosci. 3, 1488–1494.

Seidah, N.G., Benjannet, S., Pareek, S., Savaria, D., Hamelin, J., Goulet, B., Laliberte, J., Lazure, C., Chretien, M., Murphy, R.A., 1996. Cellular processing of the nerve growth factor precursor by the mammalian pro-protein convertases. Biochem. J. 314 (Pt 3), 951–960.

Shooter, E.M., 2001. Early days of the nerve growth factor proteins. Annu. Rev. Neurosci. 24, 601–629.

Soffientini, P., Bachi, A., 2016. STAGE-diging: a novel in-gel digestion processing for proteomics samples. J Proteomics 140, 48–54.

Soligo, M., Piccinin, S., Protto, V., Gelfo, F., De Stefano, M.E., Florenzano, F., Berretta, E., Petrosini, L., Nistico, R., Manni, L., 2017. Recovery of hippocampal functions and modulation of muscarinic response by electroacupuncture in young diabetic rats. Sci. Rep. 7, 9077.

Soligo, M., Protto, V., Florenzano, F., Bracci-Laudiero, L., De Benedetti, F., Chiaretti, A., Manni, L., 2015. The mature/pro nerve growth factor ratio is decreased in the brain of diabetic rats: analysis by ELISA methods. Brain Res. 1624, 455–468.

Tiveron, C., Fasulo, L., Capsoni, S., Malerba, F., Marinelli, S., Paoletti, F., Piccinin, S., Scardigli, R., Amato, G., Brandi, R., Capelli, P., D'Aguanno, S., Florenzano, F., La Regina, F., Lecci, A., Manca, A., Meli, G., Pistillo, L., Berretta, N., Nistico, R., Pavone, F., Cattaneo, A., 2013. ProNGF\NGF imbalance triggers learning and memory deficits, neurodegeneration and spontaneous epileptic-like discharges in transgenic mice. Cell Death Differ. 20, 1017–1030.

Truzzi, F., Marconi, A., Lotti, R., Dallaglio, K., French, L.E., Hempstead, B.L., Pincelli, C., 2008. Neurotrophins and their receptors stimulate melanoma cell proliferation and migration. J. Investig. Dermatol. 128, 2031–2040.

West, A.E., Pruunsild, P., Timmusk, T., 2014. Neurotrophins: transcription and translation. Handb. Exp. Pharmacol. 220, 67–100.